

Glycosylation Modulates Human CD2-CD58 Adhesion via Conformational Adjustment

Xingyu Wang,[§] Chang G. Ji,^{*,†,‡,§} and John Z. H. Zhang^{*,†,‡,§,||}

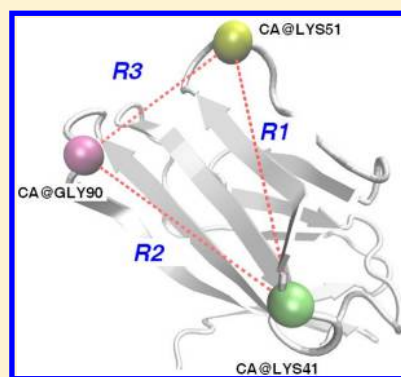
[†]Shanghai Engineering Research Center of Molecular Therapeutics and New Drug Development, School of Chemistry and Molecular Engineering, East China Normal University, Shanghai 200062, China

[‡]State Key Laboratory of Precision Spectroscopy, Institute of Theoretical and Computational Science, East China Normal University, Shanghai 200062, China

[§]NYU-ECNU Center for Computational Chemistry at NYU Shanghai, Shanghai 200062, China

^{||}Department of Chemistry, New York University, New York, New York 10003, United States

ABSTRACT: Human CD2 is a transmembrane cell surface glycoprotein found on T lymphocytes and natural killer cells and plays important roles in immune recognition. The interaction between human CD2 and its counter receptor CD58 facilitates surface adhesion between helper T lymphocytes and antigen presenting cells as well as between cytolytic effectors and target cells. In this study, the molecular effect of glycosylation of CD2 on the structure and dynamics of the CD2-CD58 adhesion complex were examined via MD simulation to help understand the fundamental mechanism of glycosylation that controls CD2-CD58 adhesion. The present result and detailed analysis revealed that the binding interaction of human CD2-CD58 is dominated by three hot spots that form a binding triangle whose topology is critical for stable binding of CD2-CD58. Our study found that the conformation of human CD2, represented by the topology of this binding triangle, is significantly adjusted and steered by glycosylation toward a particular conformation that energetically stabilizes the CD2-CD58 complex. Thus, the fundamental mechanism of glycosylation of human CD2 is to promote CD2-CD58 binding by conformational adjustment of CD2. The current result and explanation are in excellent agreement with previous experiments and help elucidate the dynamical mechanism of glycosylation of human CD2.



INTRODUCTION

Glycosylation is one of the most common cotranslational and post-translational modifications occurring in protein biosynthesis and serves a variety of structural and functional roles in membrane and secreted proteins. In eukaryotic cells, a majority of proteins synthesized in the rough endoplasmic reticulum (ER) undergo glycosylation. Glycosylation can modulate the stability and dynamics of proteins in subtle ways and plays an important role in cell–cell adhesion. CD2 is a T lymphocyte cell-adhesion molecule (CAM) found on the surface of T cells and natural killer (NK) cells. It belongs to the immunoglobulin superfamily (IgSF) which mediates adhesion of T cells to antigen-presenting cells and target cells.¹ It is the first mature T cell marker expressed in T cell ontogeny² and is one of the most extensively studied calcium-independent cell adhesion glycoproteins.³ CD2 plays essential roles in cell–cell interactions^{4,5} and signal transductions^{6,7} through interactions with its counterparts, which are CD58 in humans^{1,8,9} and CD48 in rodents.^{10–12} Structural studies of both rat^{13,14} and human CD2^{15–17} have shown that the extracellular region of CD2 consists of two immunoglobulin superfamily (IgSF) domains, a seven-stranded membrane-proximal C2-set domain and a nine-stranded NH₂-terminal adhesion domain.

The CD58 binding site of human CD2 is a localized and highly charged surface area located on the *GFCC'C''* face of the

NH₂-terminal adhesion domain (see Figure 1), which is abbreviated as HsCD2ad. This site contains relevant residues in F, C, and C' strands as well as FG, CC', and C'C'' loops and measures ~770 Å² in total surface area¹⁸ (Figure 1). NMR studies showed that fluctuations on the nanosecond to picosecond time scale are enhanced in these areas, and the CD58 binding loops are more flexible compared to other loops.^{19,20} The interaction between CD2 and CD58 has a very fast dissociation rate ($k_{\text{off}} > 4 \text{ s}^{-1}$) and thus a low binding affinity ($k_{\text{d}} \approx 10 \text{ } \mu\text{M}$ at 37 °C).²¹ Furthermore, the crystal structure of the heterophilic adhesion complex between the amino-terminal domains of human CD2 and CD58, abbreviated as HsCD2ad-CD58, reveals that their binding interface is relatively small and has poor shape complementarity.¹

In glycosylated HsCD2ad, a single high mannose glycan (Figure 2) is linked to the side chain of Asn65 on the opposite side of the CD58 binding face of HsCD2ad (Figure 1), which is crucial for its adhesion function. Experiments showed that complete removal of the glycan from HsCD2ad leads to the loss of binding to CD58 and therefore the adhesion function.²² Previous studies proposed a mechanism that the glycan can

Received: October 1, 2014

Revised: May 18, 2015

Published: May 18, 2015

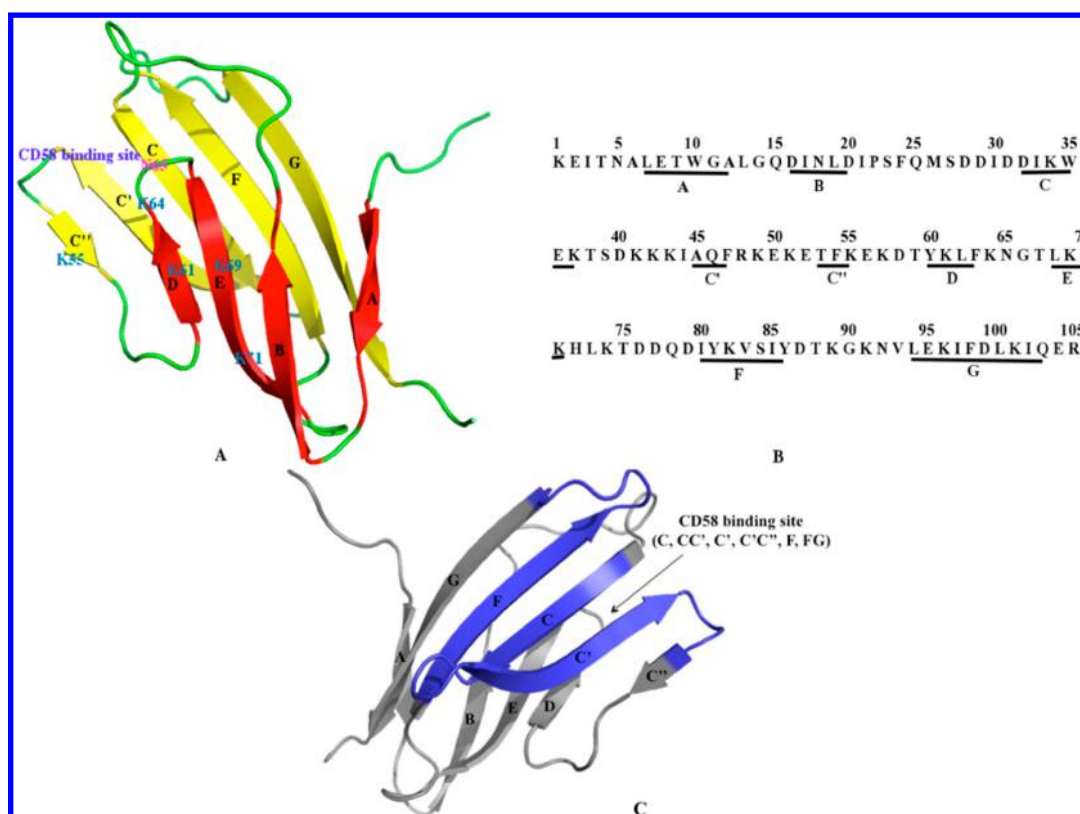


Figure 1. (A) Ribbon diagram representation of HsCD2ad monomer (PDB code 1GYA). β strands are labeled with letters A, B, C, C', C'', D, E, F, and G. The CD58 binding site contains relevant residues in strands C, C', and F as well as loops CC', C'C'', and FG. Thus, strands C'', C', C, F, and G are directly related to the CD58 binding face and are highlighted in yellow. Strands A, B, E, and D are located on the opposite side of the binding interface and are colored in red. The N-glycan attached Asn65 is highlighted in pink. The clustering of positively charged residues Lys55, Lys61, Lys64, Lys69, and Lys71 is highlighted in blue.²³ (B) Sequence of HsCD2ad. The β strands are labeled according to an Ig V domain (strand A, residues 7–12; strand B, residues 16–20; strand C, residues 32–37; strand C', residues 45–47; strand C'', residues 53–55; strand D, residues 60–63; strand E, residues 68–71; strand F, residues 80–86; strand G, residues 94–103).¹⁷ (C) The CD58 binding site (C, CC', C', C'C'', F, FG) is highlighted in blue at the ribbon diagram of HsCD2ad monomer.

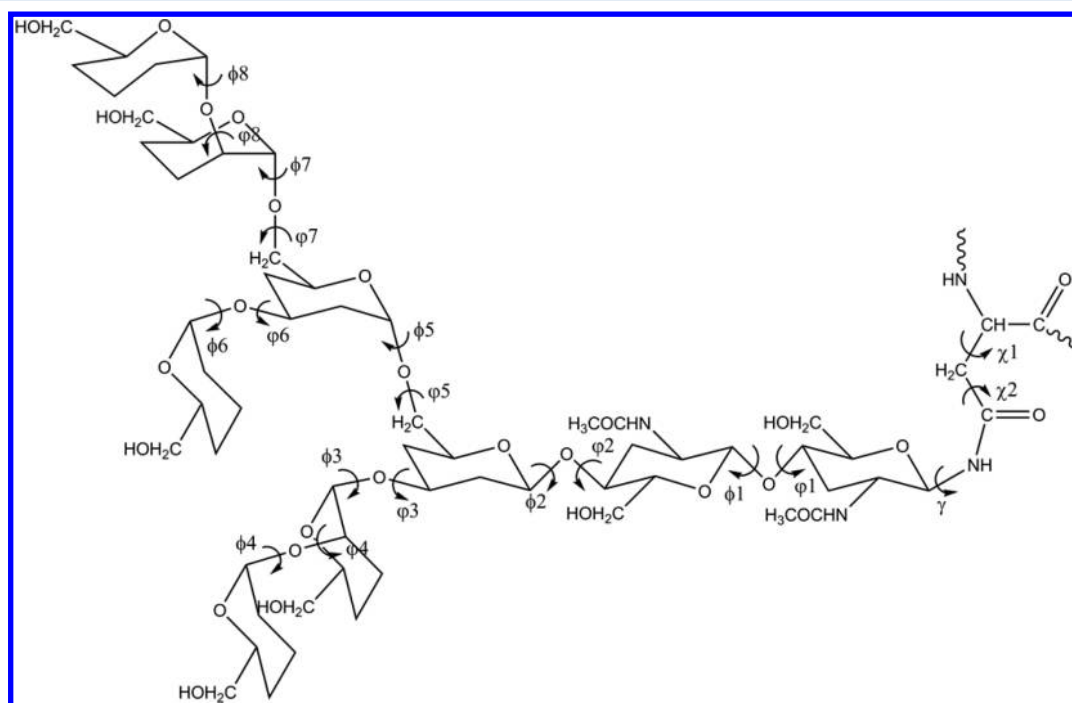


Figure 2. Chemical structure of the high-mannose N-glycan attached to Asn65. Dihedral angles (both ϕ and ψ) along with the glycosidic dihedral angle γ and the χ angles of the Asn65 side chain are labeled.

stabilize a clustering of positive charges (centered in Lys61 and surrounded by Lys55/Lys64/Lys69/Lys71) on the DEB face through hydrogen bonds, van der Waals, and entropic contributions.²³ Kelly and co-workers performed experimental studies that showed the Phe65 and Thr67 are essential in the glycosylated region.²⁴ Our previous theoretical result also confirmed the importance of these two amino acids in N-glycosylation.²⁵ More recently, Kearney and co-workers indicated that the HsCD2ad-CD58 binding process is accompanied by energetically significant conformational adjustments.²⁶ These studies provided important information toward understanding the fundamental mechanism by which glycosylation impacts the CD2 conformation and thus its interaction with CD58. It is thus desirable to further investigate detail molecular interaction and mechanism that directly affect or control the adhesion function of HsCD2ad.

In order to explore the functional role and understand the fundamental molecular mechanism of glycosylation responsible for controlling the adhesion function of HsCD2ad, detailed study of the structure and dynamics of glycoprotein as well as its nonglycosylated counterpart is needed. Since current experimental approach is largely limited in detecting dynamic structure of proteins in solution at high resolution, computational approach provides a useful tool in studying molecular mechanism at atomic resolution. In the present work, molecular dynamics (MD) simulation and detailed analysis have been carried out to study structural dynamics of HsCD2ad monomer and HsCD2ad-CD58 complex. Specifically, we studied the conformational changes at binding interfaces for both glycosylated and nonglycosylated HsCD2ad-CD58 complexes, and in particular, how those conformation changes affect the binding of CD58.

MATERIALS AND METHODS

Initial Structures. To carry out our study, we need four initial structures: glycosylated and nonglycosylated HsCD2ad monomers and HsCD2ad-CD58 complexes. First, the NMR structure of glycosylated HsCD2ad monomer (PDB code 1GYA²³) and crystal structure of nonglycosylated HsCD2ad-CD58 complex (PDB code 1QA9¹) were obtained from Protein Data Bank (www.pdb.org). The glycan is removed from glycosylated HsCD2ad monomer to obtain the nonglycosylated monomer structure. Three missing residues were added to HsCD2ad, which were Lys¹, Glu², and Ile³. The crystal structure 1QA9 is for mutant CD2-CD58 complex. In our approach, we performed demutation (Glu61Lys, Leu63Phe, and Ala67Thr on HsCD2, and Ser1Phe, Lys9Val, Gln21Val, Lys58Val, Ser85Thr, and Gly93Leu on CD58) from this structure to obtain the complex structure of the WT CD2-CD58 for simulation study. Then, the same glycan was attached to Asn⁶⁵ of HsCD2ad in the complex to obtain the glycosylated complex structure of HsCD2ad-CD58. Table 1 lists all the abbreviations used in the present simulation of various systems. Crystal water molecules were placed by using 3D-RISM²⁷ method.

MD Simulations. Molecular dynamics (MD) simulations were performed using double precision GROMACS simulation package (www.gromacs.org).²⁸ Systems were solvated in rhombic dodecahedron TIP3P water box and neutralized by adding counterions. Periodic boundary conditions and the particle mesh Ewald²⁹ methods were used for long-range electrostatic effects. Prior to MD simulations, systems were energy minimized to avoid any steric conflicts generated during

Table 1. Structures Used for Molecular Dynamics Simulation

NH ₂ -Terminal Adhesion Domain of Human CD2 Monomer	
HsCD2ad	no glycan
HsCD2ad (g)	glycan
Complex between the NH ₂ -Terminal Adhesion Domains of Human CD2 and CD58	
HsCD2ad(ng)-CD58	no glycan
HsCD2ad(g)-CD58	glycan

the setup. For MD simulation, integration time step was 2 fs. The SHAKE algorithm³⁰ was employed to constrain bond lengths containing hydrogen atoms. 100 ps NVT and 10 ns NPT equilibrations were performed, and then 200 and 250 ns productions runs were carried out for monomers and complexes, respectively. Amber99SB force field³¹ and GLYCAM06 force field³² were used for proteins and carbohydrates. These two force fields are designed to be compatible with each other,³³ and their combination has been successfully used in several studies of carbohydrate–protein complexes and glycoproteins.^{34–37}

RESULTS AND DISCUSSION

Nonglycosylated HsCD2ad Does Not Bind Well with CD58. Human CD2 dynamically binds to its counter receptor CD58, which promotes the initial stages of T cell contact with antigen presenting cells (APCs) or target cells. Unlike in integrin-based adhesion, CD2-CD58 binding interaction is independent of T cell receptor (TCR) triggering. This process fosters immune recognition reactions such as TCR-peptide/major histocompatibility complex (pMHC)³ or NK receptor–MHC interactions and plays an important role in T cell activation.^{38,39} Previous experimental studies find that N-glycosylation in the adhesion domain of human CD2 is required for its immune adhesion function. Without glycosylation, human CD2 could not bind well with CD58 and may undermine T cell response.

The human CD2 and CD58 bind in an asymmetric and orthogonal fashion. Their binding interface contains major β sheets within immunoglobulin-like adhesion domains.¹ For most protein–protein interactions, the binding affinity is not evenly distributed across interfaces. Instead, hot spots make dominant contributions to the free energy of binding.⁴⁰ In the HsCD2ad-CD58 complex, three main binding hot spots are located at the dimer interface, which are highlighted in Figure 3. Loop1 contains Lys41 and Lys43 of HsCD2ad, and Glu25 and Asp84 of CD58. Loop2 includes Arg48, Lys51 of HsCD2ad and Glu39, Glu42, Asn51 of CD58. Several hydrogen bonds and salt bridges are formed between these amino acids. From the HsCD2ad side, the only hydrophobic contact is in loop3,⁴¹ involving the packing of the aromatic ring of HsCD2ad Tyr86 with the aliphatic portion of CD58 Lys34.

To investigate the dynamic stability of HsCD2ad-CD58 complex, two simulations were performed in this work, i.e., simulations of glycosylated HsCD2ad-CD58 complex and nonglycosylated HsCD2ad-CD58 complex in water. The glycosylated complex (HsCD2ad(g)-CD58) was stable during the entire 250 ns of simulation. For nonglycosylated HsCD2ad(ng)-CD58, the binding partners moved away from each other during the simulation and the final complex structure was loosened as shown in Figure 4. Distances between the centroids of CD2 and CD58 are shown in Figure 5. When glycan was not presented, the two parts moved further

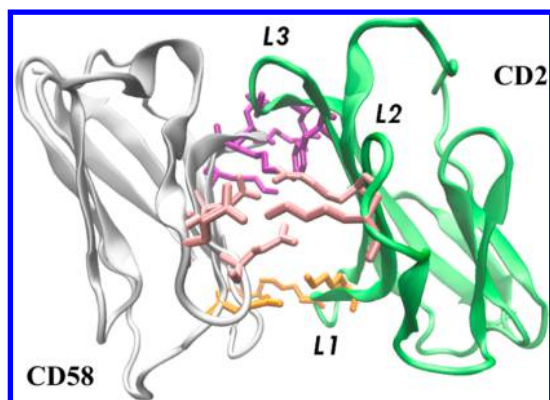


Figure 3. Crystal structure of HsCD2ad-CD58 complex (PDB code 1QA9). Three main binding hot spots are highlighted in yellow, pink, and purple. Loop 1: residues Lys41, Lys43 of HsCD2ad and residues Glu25, Asp84 of CD58. Loop 2: residues Arg48, Lys51 of HsCD2ad and residues Glu39, Glu42, Asn51 of CD58. Loop 3: residues Tyr86, Gly90, Asn92 of HsCD2ad and residues Lys32, Asp33, Lys34 of CD58.

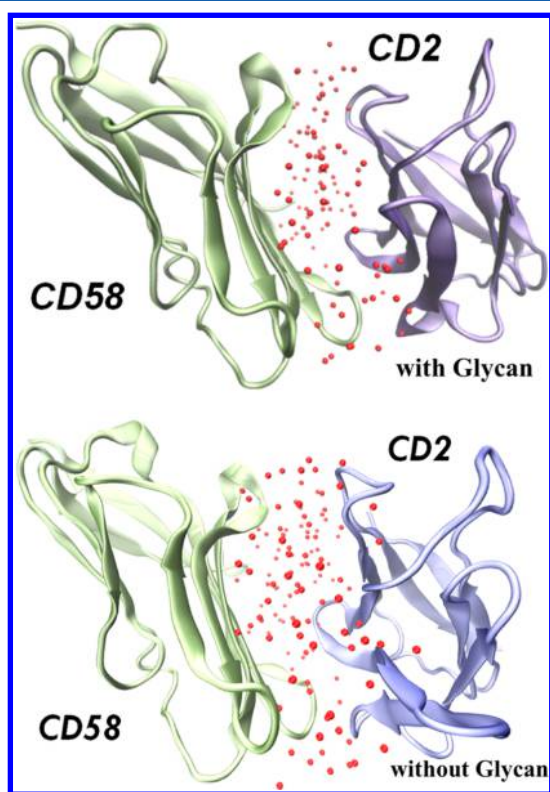


Figure 4. Final structure of HsCD2ad(g)-CD58 complex (upper figure) and HsCD2ad(ng)-CD58 complex (lower figure) from MD simulation. Water molecules are represented by small red balls. As shown in the figure, there are more interfacial waters in nonglycosylated complex of HsCD2ad(ng)-CD58 (lower figure), indicating weak binding.

by 1 Å after 150 ns simulation time. From Figure 4, it is clear that part of the protein–protein interactions within the binding interface was replaced by interactions with water molecules. The water molecules within the HsCD2ad(ng)-CD58 complex were analyzed, and Figure 6 plots the number of water molecules within the HsCD2ad-CD58 complex, in both glycosylated and nonglycosylated forms, as a function of simulation time. The number of these interface water molecules

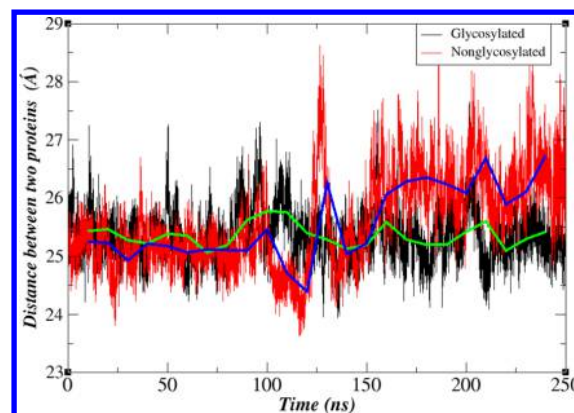


Figure 5. Distances between the centroids of CD2 and CD58 for HsCD2ad(ng)-CD58 complex (red) and HsCD2ad(g)-CD58 complex (black). The blue and green lines are their averaged values, respectively.

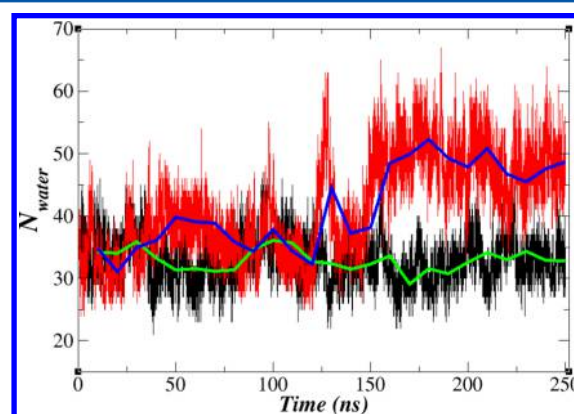


Figure 6. Number of interfacial water molecules as a function of simulation time for HsCD2ad(ng)-CD58 complex (red) and HsCD2ad(g)-CD58 complex (black). The blue and green lines are their averaged values, respectively.

in the glycosylated HsCD2ad(g)-CD58 complex was relatively stable during the entire 250 ns simulation, indicating a stable binding structure. In contrast, the number of water increased dramatically after 150 ns in the nonglycosylated HsCD2ad(ng)-CD58 complex. This result suggests that some interprotein interactions between HsCD2ad and CD58 observed in the crystal structure were interrupted during the simulation and a large amount of water molecules rushed into the binding interface.

Since most of the interactions between HsCD2ad and CD58 are hydrogen bonds and salt bridges, the number of hydrogen bonds across the binding interface in HsCD2ad(ng)-CD58 complex is plotted in Figure 7. As shown in the figure, the number of hydrogen bonds was decreased to a lower value after 150 ns of simulation, indicating weaker binding in the interface for nonglycosylated complex. The result is consistent with the above analysis.

Correlated Motion between Glycosyl and HsCD2ad.

Protein's global dynamics is determined by protein's native structure and dynamic interactions among residues. When glycan was attached to HsCD2ad, new interactions between glycan and the protein were added to the original interaction network, which may influence equilibrium structure and internal dynamics of the protein. Here we investigate in detail the correlated motions between glycan and individual protein

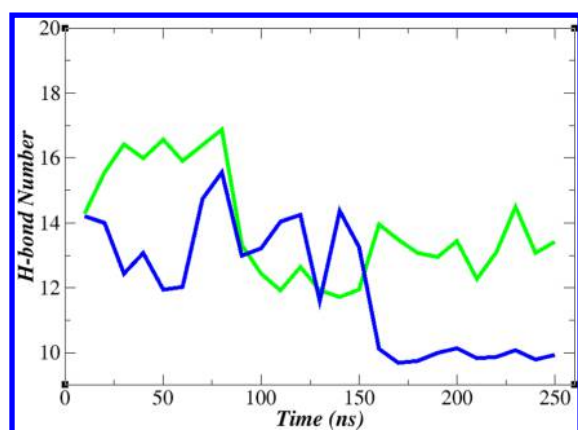


Figure 7. Number of hydrogen bonds across the binding surface as a function of simulation time in the HsCD2ad-CD58 complex (green, glycosylated form; blue, nonglycosylated form). Each point was averaged over 10 ns simulation time.

residues of HsCD2ad through dynamical cross-correlation analysis. Dynamical cross-correlation matrix (DCCM) is a three-dimensional matrix representation that graphically displays time-correlated information among the residues of the protein. For each pair of C- α atoms i on HsCD2ad and oxygen atoms j on the attached glycan, the cross-correlation coefficient is given by

$$C_{ij} = \frac{\langle \Delta r_i \Delta r_j \rangle}{(\langle \Delta r_i^2 \rangle \langle \Delta r_j^2 \rangle)^{1/2}}$$

where Δr_i is the displacement from the mean position of the i th atom and the symbol $\langle \rangle$ represents time average over the MD trajectory. The magnitudes of all pairwise cross-correlation coefficients are plotted to assess the atomic fluctuations/displacements of the systems.^{42,43} On the DCCM map, each point represents a correlation C_{ij} of atoms i and j . If $C_{ij} = 1$, the fluctuations of atoms i and j are completely correlated (same period and same phase). If $C_{ij} = -1$, the fluctuations of atoms i and j are completely anticorrelated (same period and opposite phase). If $C_{ij} = 0$, the fluctuations of atoms i and j are not correlated. In our analysis, atoms i and j are regarded as correlated if C_{ij} value is substantially different from zero.

The correlation dynamics between glycan and the protein analyzed from 250 ns simulation is plotted in Figure 8 as two-

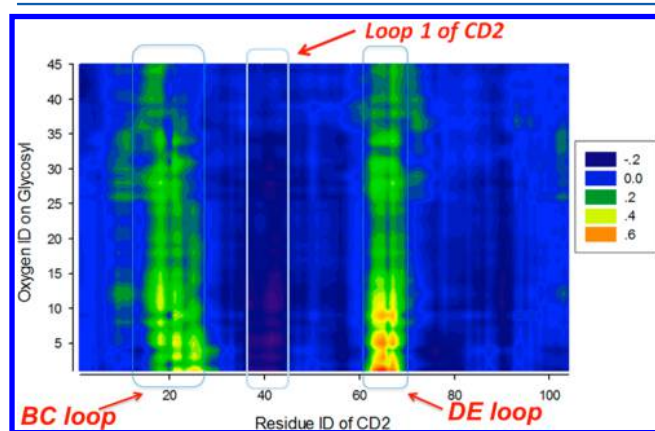


Figure 8. Heat map of dynamic cross-correlation matrix (DCCM) between oxygen atoms of glycan and C α atoms of CD2.

dimensional heat map. Figure 8 shows that three regions (residues 20–25, residue 38–42, and residues 62–67) of the protein are strongly correlated with glycan. As for residues 38–42, this region corresponds to loop 1 of the protein, which is recognized as one of the binding hot spots with CD58. It should be noted that glycan is actually attached to the opposite side of the CD2/CD58 binding surface. Thus, glycan does not directly participate in protein–protein interaction. Nevertheless, the dynamical motion between glycan and one of the binding hot spot of CD2 (loop1) is strongly correlated. Although loop1 of CD2 is located far away from glycan (about 10 Å away), their dynamical behaviors are strongly connected through the complex intraprotein interaction network. As for residues 62–67 (DE loop), the correlation coefficient is highly positive because the glycan is chemically bonded to residue 65. DE loop may play an important role in communicating glycan motions to the CD58 binding face, since it is connected with glycan directly. To identify whether DE loop dynamics are correlated with motions of residues on the CD58 binding face, correlation maps associated with three representative residues of DE loop (Phe63, Gly66, and Thr67) are projected out and plotted in Figure 9. Figure 9 shows that dynamics of DE loop

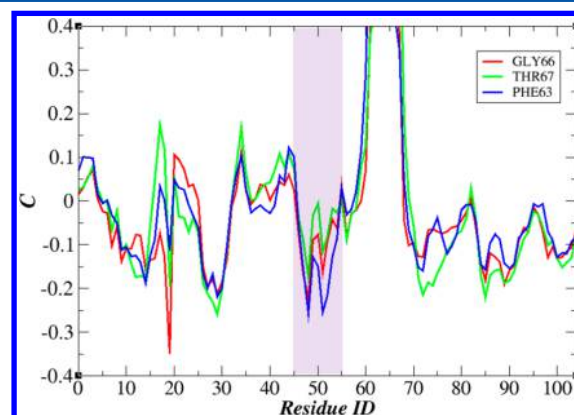


Figure 9. CD2 dynamical correlation map associated with residues Phe63, Gly66, and Thr67.

and residues 46–55 are strongly correlated. Residues 46–55 are located on the second binding hot spot loop 2 (see Figure 4). As for residues 20–25 (BC loop), this region also has strong positive correlation with glycan. The dynamic correlation coefficients between BC loop and other residues, shown in Figure 10, indicate that motions of residues 84–92 are strongly correlated with BC loop. Residues 84–92 are located on the third binding hot spot loop 3 (see Figure 4). These data suggest that BC and DE loop dynamics are correlated with motions of hot spot residues on the CD58 binding face.

There are many hydrogen bond donor and acceptor atoms in glycan, and glycan interacts with protein residues mainly through hydrogen bond interaction. To investigate why their motions were correlated during MD simulation, closer examination of direct hydrogen bond interactions between glycan and CD2 was performed. The glycan residues were very flexible and the hydrogen bonds formed between glycan and the protein break frequently during MD simulation. Glycan residues formed hydrogen bonds with different protein residues at different times. Occupancy of these hydrogen bonds during MD simulation was analyzed and mapped on protein's residue (see Figure 11). From Figure 11 we may find that glycan

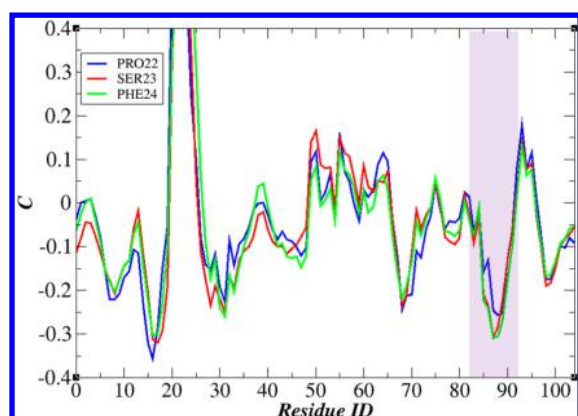


Figure 10. CD2 dynamical correlation map associated with residues Pro22, Ser23, and Phe24.

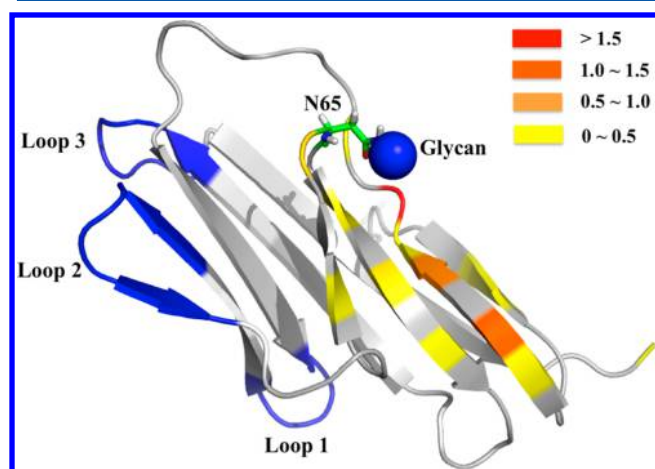


Figure 11. Occupancy of hydrogen bonds formed between glycan and different protein residues during MD simulation. If there are hydrogen bonds formed between the protein residue and glycan, that protein residue is shown in color. The higher is the percentage occupancy of hydrogen bonds formed by the certain protein residue, the more reddish it is. Sales at the right side of the figure indicate the total percentage occupancy of hydrogen bonds for each residue. Loop 1, loop 2, and loop 3 are highlighted in blue. Asn65 is shown as sticks. Glycan is represented by the blue ball.

interacts with Asp16, Asn18, Asp20, Lys64, and Lys69 directly. These “hot residues” may be responsible for bridging motions of glycan and CD2’s binding interface.

Since their dynamics are correlated, we anticipate that structural distribution of CD2 binding interface and the whole protein may be affected by the attached glycan. Thus, it is informative to analyze protein structural change due to glycosylation.

Effect of Glycosylation on Conformational Ensemble of HsCD2ad. Two independent simulations of apo-glycosylated HsCD2ad and apo-nonglycosylated HsCD2ad were performed to investigate how glycan affects HsCD2ad’s structure ensemble in solution. HsCD2ad binds CD58 mainly through three loops as pictured in Figure 3. The geometry of their relative positions can be used as a good reaction coordinate to represent conformational ensemble of HsCD2ad on the binding interface. To facilitate the quantitative measure of our structural analysis, three Ca atoms within the three hot spots, Ca@Lys41 , Ca@Lys51 , and Ca@Gly90 , were chosen to define a triangle as shown in Figure 12. Distances between each

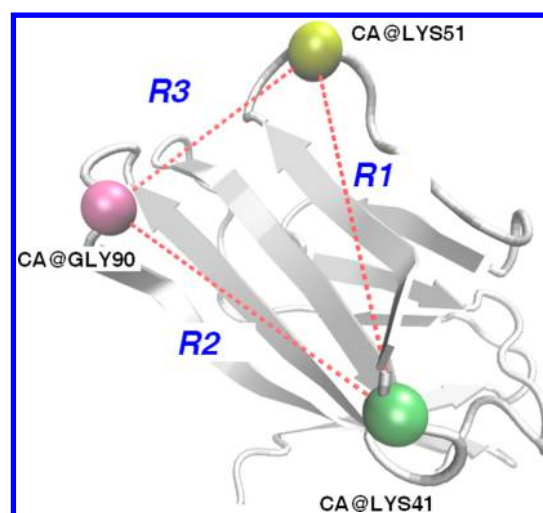


Figure 12. Relative positions of three binding hot spots on the apo-HsCD2ad binding interface. Ca atoms of Lys41, Lys51 and Gly90 are colored in green, yellow, and pink. Distances ($R1$, $R2$, $R3$) between each pair of these three amino acids are highlighted in red dash lines.

pair of these three atoms were measured, and their distributions are plotted in Figure 13. For comparison, geometric parameters

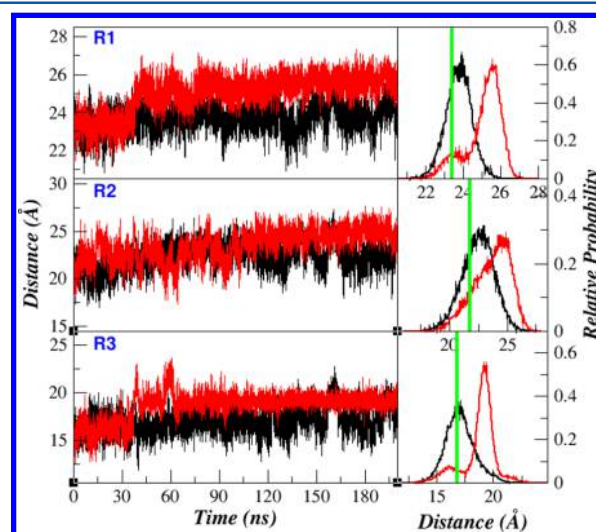


Figure 13. Left side: length (unit, Å) of $R1$, $R2$, and $R3$ as a function of simulation time. Right side: length distributions. Red: apo-HsCD2ad(ng). Black: apo-HsCD2ad(g). Green: HsCD2ad-CD58 crystal structure.

derived from crystal structure of HsCD2ad-CD58 complex are highlighted in green. From Figure 13, we find that the most sampled $R1$, $R2$, and $R3$ lengths for glycan-form apo-HsCD2ad stayed very close to those in the complex form. However, the distribution of their relative position in nonglycosylated apo-HsCD2ad(ng) deviated significantly from the complex form. The area of the triangle formed by Ca@Lys41 , Ca@Lys51 , and Ca@Gly90 was also measured (see Figure 14). The averaged area of the triangle for apo-HsCD2ad is 181 and 209 Å² for the glycosylated and nonglycosylated forms, respectively. In the HsCD2ad/CD58 complex, the area of this triangle is about 175 Å². Without glycosylation, the triangle formed by three hot spots is about 15% larger than the conformation in the complex. This indicates that the three binding hot spots of

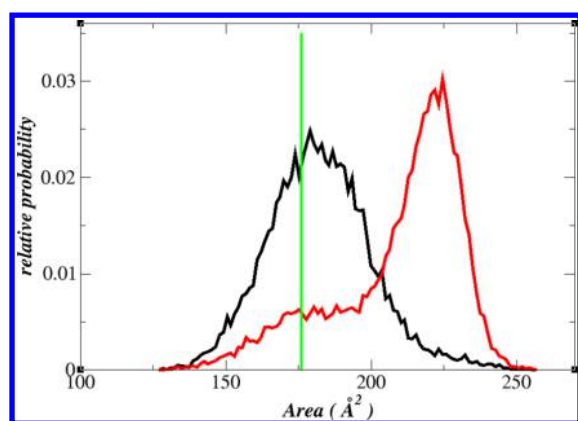


Figure 14. Area distributions of the triangle formed by Ca@Lys41 , Ca@Lys51 , and Ca@Gly90 during MD simulation. Red: apo-HsCD2ad(ng). Black: apo-HsCD2ad(g). Green: HsCD2ad-CD58 crystal structure.

HsCD2ad cannot fit well CD58 simultaneously when glycan is not attached.

The free energy landscapes of apo-HsCD2ad are constructed in Figure 15. Free energies were obtained by using the formula

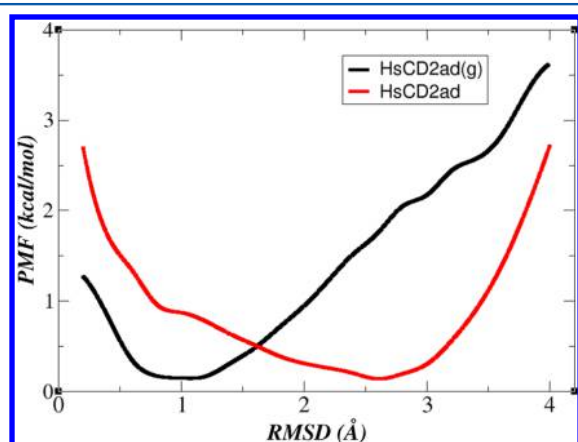


Figure 15. Free energy landscapes of apo-HsCD2ad calculated as a function of root-mean-square deviation (rmsd) of R1, R2, and R3 in apo-HsCD2ad during the simulation from HsCD2ad-CD58 crystal structure. $\text{PMF}(dG) = -kT \ln(H(\text{rmsd}))$, where $H(\text{rmsd})$ is the histogram of rmsd, rmsd is the root-mean-square deviation of R1, R2, and R3 in apo HsCD2ad from HsCD2ad-CD58 complex during MD simulations. $\text{rmsd} = \{[(R1 - R1_c)^2 + (R2 - R2_c)^2 + (R3 - R3_c)^2]/3\}^{1/2}$. $R1_c$, $R2_c$, and $R3_c$ are lengths in HsCD2ad-CD58 crystal structure.

$G(\text{rmsd}) = -kT \ln(H(\text{rmsd}))$, where $H(\text{rmsd})$ is the histogram of rmsd,

$$\text{rmsd} = \{[(R1 - R1_c)^2 + (R2 - R2_c)^2 + (R3 - R3_c)^2]/3\}^{1/2}$$

where $R1_c$, $R2_c$, and $R3_c$ are lengths in the HsCD2ad-CD58 crystal structure. The free energy landscape suggests that most sampled structures in glycosylated apo-HsCD2ad are very close to the one in HsCD2ad-CD58 complex, but they were far away in the case of nonglycosylated apo-HsCD2ad.

CONCLUSION

In the present study, long time MD simulations in explicit solvent environment of HsCD2ad monomer and HsCD2ad-CD58 complex were performed and detailed dynamical analysis was carried out for both glycan- and non-glycan forms. In the HsCD2ad-CD58 complex, the nonglycosylated apo-HsCD2ad, does not bind well with its counter receptor CD58. The HsCD2ad(ng)-CD58 complex undergoes a larger conformational drift during the MD simulation. Hydrogen bonds between HsCD2ad(ng) and CD58 were undermined and water molecules were pushed into the binding interface after 150 ns simulation time. Detailed DCCM analysis shows that dynamic motions of glycans and one of the binding hotspots of CD2 are strongly correlated. Geometric analysis and examination of free energy landscape of apo-HsCD2ad indicated that most sampled structures in glycosylated apo-HsCD2ad are very close to the one in HsCD2ad-CD58 crystal structure. However, the structure of nonglycosylated apo-HsCD2ad deviates significantly from its bounded form. These data suggest that the glycan-form apo-HsCD2ad structure was prepared for binding with CD58.

Here a simple mechanism that may explain how glycosylation governs HsCD2ad's biological function is proposed as the following. The schematic description is shown in Figure 16.

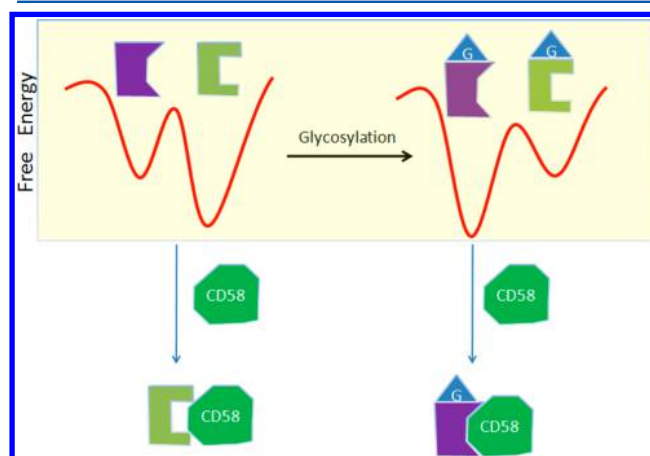


Figure 16. Schematic description of the running model.

Glycosylation point (Asn⁶⁵) is located on the opposite side of the CD58 binding site (see Figure 1), so the glycan does not interact with CD58 directly. Instead, the glycosylation plays a critical role in modulating HsCD2ad's dynamics and conformational ensemble. When HsCD2ad is nonglycosylated, energetically favorable conformational ensemble of HsCD2ad is far away from the bounded form and HsCD2ad does not fit well with CD58. After glycosylation, however, interaction network in HsCD2ad changes and conformational ensemble of HsCD2ad is shifted toward that that favorable for binding to CD58. Thus, glycosylation modulates human CD2-CD58 adhesion by adjusting CD2 conformation.

AUTHOR INFORMATION

Corresponding Authors

*C.G.J.: e-mail, chicago.ji@gmail.com.

*J.Z.H.Z.: e-mail, john.zhang@nyu.edu.

Notes

The authors declare no competing financial interest.

ACKNOWLEDGMENTS

We thank the National Natural Science Foundation of China (Grants 21003048 and 21433004), Shanghai Natural Science Foundation (Grant 14ZR1411900), and Shanghai Putuo District (Grant 2014-A-02) for financial support. C.G.J. is also supported by “the Fundamental Research Funds for the Central Universities” and Open Research Fund of the State Key Laboratory of Precision spectroscopy, East China Normal University. We also thank the Supercomputer Center of ECNU for providing us computational time.

REFERENCES

- (1) Wang, J. H.; Smolyar, A.; Tan, K.; Liu, J. H.; Kim, M.; Sun, Z. Y.; Wagner, G.; Reinherz, E. L. Structure of a heterophilic adhesion complex between the human CD2 and CD58 (LFA-3) counter-receptors. *Cell* **1999**, *97*, 791–803.
- (2) Sayre, P. H.; Reinherz, E. L. Structure and function of the erythrocyte receptor CD2 on human T lymphocytes: a review. *Scand. J. Rheumatol., Suppl.* **1988**, *76*, 131–144.
- (3) Wang, J. H.; Reinherz, E. L. Structural basis of cell-cell interactions in the immune system. *Curr. Opin. Struct. Biol.* **2000**, *10*, 656–661.
- (4) Kamoun, M.; Martin, P. J.; Hansen, J. A.; Brown, M. A.; Siadak, A. W.; Nowinski, R. C. Identification of a human T lymphocyte surface protein associated with the E-rosette receptor. *J. Exp. Med.* **1981**, *153*, 207–212.
- (5) Davis, S. J.; Merwe, P. A. v. d. Structure and ligand interactions of CD2 implications for T-cell function. *Immunol. Today* **1996**, *17*, 177–187.
- (6) Meuer, S. C.; Hussey, R. E.; Fabb, M.; Fox, D.; Acuto, O.; Fitzgerald, K. A.; Hodgdon, J. C.; Protentis, J. P.; Schlossman, S. F.; Reinherz, E. L. An alternative pathway of T-cell activation: a functional role for the 50 kd T11 sheep erythrocyte receptor protein. *Cell* **1984**, *36*, 897–906.
- (7) Beyers, A. D.; Barclay, A. N.; Law, D. A.; He, Q.; Williams, A. F. Activation of T lymphocytes via monoclonal antibodies against rat cell surface antigens with particular reference to CD2 antigen. *Immunol. Rev.* **1989**, *111*, 59–77.
- (8) Shaw, S.; Luce, G. E. G.; Quinones, R.; Cress, R. E.; Springer, T. A.; Sanders, M. E. Two antigen-independent adhesion pathways used by human cytotoxic T-cell clones. *Nature* **1986**, *323*, 262–264.
- (9) Ikemizu, S.; Sparks, L. M.; Merwe, P. A. v. d.; Harlos, K.; Stuart, D. I.; Jones, E. Y.; Davis, S. J. Crystal structure of the CD2-binding domain of CD58 (lymphocyte function-associated antigen 3) at 1.8-Å resolution. *Proc. Natl. Acad. Sci. U.S.A.* **1999**, *96*, 4289–4294.
- (10) Evans, E. J.; Castro, M. A. A.; O'Brien, R.; Kearney, A.; Walsh, H.; Sparks, L. M.; Tucknott, M. G.; Davies, E. A.; Carmo, A. M.; Merwe, P. A. v. d.; et al. Crystal structure and binding properties of the CD2 and CD244 (2B4)-binding protein, CD48. *J. Biol. Chem.* **2006**, *281*, 29309–29320.
- (11) Kato, K.; Koyanagi, M.; Okada, H.; Takanashi, T.; Wong, Y. W.; Williams, A. F.; Okumura, K.; Yagita, H. CD48 is a counter-receptor for mouse CD2 and is involved in T cell activation. *J. Exp. Med.* **1992**, *176*, 1241–1249.
- (12) Merwe, P. A. v. d.; McPherson, D. C.; Brown, M. H.; Barclay, A. N.; Cyster, J. G.; Williams, A. F.; Davis, S. J. The NH2-terminal domain of rat CD2 binds rat CD48 with a low affinity and binding does not require glycosylation of CD2. *Eur. J. Immunol.* **1993**, *23*, 1373–1377.
- (13) Driscoll, P. C.; Cyster, J. G.; Campbell, I. D.; Williams, A. F. Structure of domain 1 of rat T lymphocyte CD2 antigen. *Nature* **1991**, *353*, 762–765.
- (14) Jones, E. Y.; Davis, S. J.; Williams, A. F.; Harlos, K.; Stuart, D. I. Crystal structure at 2.8 Å resolution of a soluble form of the cell adhesion molecule CD2. *Nature* **1992**, *360*, 232–239.
- (15) Bodian, D. L.; Jones, E. Y.; Harlos, K.; Stuart, D. I.; Davis, S. J. Crystal structure of the extracellular region of the human cell adhesion molecule CD2 at 2.5 Å resolution. *Structure* **1994**, *2*, 755–766.
- (16) Withka, J. W.; Wyss, D. F.; Wagner, G.; Arulanandam, A. R.; Reinherz, E. L.; Recny, M. A. Structure of the glycosylated adhesion domain of human T lymphocyte glycoprotein CD2. *Structure* **1993**, *1*, 69–81.
- (17) Wyss, D. F.; Withka, J. M.; Knoppers, M. H.; Sterne, K. A.; Recny, M. A.; Wagner, G. Proton resonance assignments and secondary structure of the 13.6 kDa glycosylated adhesion domain of human CD2. *Biochemistry* **1993**, *32*, 10995–11006.
- (18) Arulanandam, A. R.; Withka, J. M.; Wyss, D. F.; Wagner, G.; Kister, K.; Pallai, P.; Recny, M. A.; Reinherz, E. L. The CD58 (LFA-3) binding site is a localized and highly charged surface area on the AGFCC' C" face of the human CD2 adhesion domain. *Proc. Natl. Acad. Sci. U.S.A.* **1993**, *90*, 11613–11617.
- (19) Wyss, D. F.; Dayie, K. T.; Wagner, G. The counterreceptor binding site of human CD2 exhibits an extended surface patch with multiple conformations fluctuating with millisecond to microsecond motions. *Protein Sci.* **1997**, *6*, 534–542.
- (20) Kitao, A.; Wagner, G. A space-time structure determination of human CD2 reveals the CD58-binding mode. *Proc. Natl. Acad. Sci. U.S.A.* **2000**, *97*, 2064–2068.
- (21) Merwe, P. A. v. d.; Barclay, A. N.; Mason, D. W.; Davies, E. A.; Morgan, B. P.; Tone, M.; Krishnam, A. K.; Ianelli, C.; Davis, S. J. Human cell-adhesion molecule CD2 binds CD58 (LFA-3) with a very low affinity and an extremely fast dissociation rate but does not bind CD48 or CD59. *Biochemistry* **1994**, *33*, 10149–10160.
- (22) Recny, M. A.; Luther, M. A.; Knoppers, M. H.; Neidhardt, E. A.; Khandekar, S. S.; Concino, M. F.; Schlömk, P. A.; Francis, M. A.; Moebius, U.; Reinhold, B.; et al. N-glycosylation is required for human CD2 immunoadhesion functions. *J. Biol. Chem.* **1992**, *267*, 22428–22434.
- (23) Wyss, D. F.; Choi, J. S.; Li, J.; Knoppers, M. H.; Willis, K. J.; Arulanandam, A. R.; Smolyar, A.; Reinherz, E. L.; Wagner, G. Conformation and function of the N-linked glycan in the adhesion domain of human CD2. *Science* **1995**, *269*, 1273–1278.
- (24) Culyba, E. K.; Price, J. L.; Hanson, S. R.; Dhar, A.; Wong, C.-H.; Gruebele, M.; Powers, E. T.; Kelly, J. W. Protein native state stabilization by placing aromatic side chains in N-glycosylated reverse turns. *Science* **2011**, *331*, 571–575.
- (25) Wang, X. Y.; Ji, C. G.; Zhang, J. Z. H. Exploring the molecular mechanism of stabilization of the adhesion domains of human CD2 by N-glycosylation. *J. Phys. Chem. B* **2012**, *116*, 11570–11577.
- (26) Kearney, A.; Avramovic, A.; Castro, M. A. A.; Carmo, A. M.; Davis, S. J.; Merwe, P. A. v. d. The contribution of conformational adjustments and long-range electrostatic forces to the CD2/CD58 interaction. *J. Biol. Chem.* **2007**, *282*, 13160–13166.
- (27) Luchko, T.; Gusarov, S.; Roe, D. R.; Simmerling, C.; Case, D. A.; Tuszynski, J.; Kovalenko, A. Three-dimensional molecular theory of solvation coupled with molecular dynamics in Amber. *J. Chem. Theory Comput.* **2010**, *6*, 607–624.
- (28) Hess, B. GROMACS 4: algorithms for highly efficient, load-balanced, and scalable molecular simulation. *J. Chem. Theory Comput.* **2008**, *4*, 435–447.
- (29) Darden, T.; York, D.; Pedersen, L. Particle mesh Ewald: An N-log(N) method for Ewald sums in large systems. *J. Chem. Phys.* **1993**, *98*, 10089–10092.
- (30) Ryckaert, J. P.; Ciccotti, G.; Berendsen, H. J. C. Numerical integration of the Cartesian equations of motion of a system with constraints: molecular dynamics of n-alkanes. *J. Comput. Phys.* **1977**, *23*, 327–341.
- (31) Hornak, V.; Abel, R.; Okur, A.; Strockbine, B.; Roitberg, A.; Simmerling, C. Comparison of multiple Amber force fields and development of improved protein backbone parameters. *Protein* **2006**, *65*, 712–725.
- (32) Kirschner, K. N.; Yongye, A. B.; Tschampel, S. M.; Gonzalez-Outeirino, J.; Daniels, C. R.; Foley, B. L.; J, W. R. GLYCAM06: A

generalizable biomolecular force field. Carbohydrates. *J. Comput. Chem.* **2008**, *29*, 622–655.

(33) Case, D. A.; Darden, T. A.; Cheatham, T. E., III; Simmerling, C. L.; Wang, J.; Duke, R. E.; Luo, R.; Walker, R. C.; Zhang, W.; Merz, K. M.; et al. *AMBER 11*; University of California: San Francisco, CA, 2010.

(34) DeMarco, M. L.; Woods, R. J. Structural biology: a game of snakes and ladders. *Glycobiology* **2008**, *18*, 426–440.

(35) Guardiani, C.; Signorini, G. F.; Livi, R.; Papini, A. M.; Procacci, P. Conformational landscape of n-glycosylated peptides detecting autoantibodies in multiple sclerosis, revealed by hamiltonian replica exchange. *J. Phys. Chem. B* **2012**, *116*, 5458–5467.

(36) Yao, J.; Nellas, R. B.; Glover, M. M.; Shen, T. Stability and sugar recognition ability of ricin-like carbohydrate binding domains. *Biochemistry* **2011**, *50*, 4097–4104.

(37) Islam, S. M.; Richards, M. R.; Taha, H. A.; Byrns, S. C.; Lowary, T. L.; Roy, P.-N. Conformational analysis of oligoarabinofuranosides: overcoming torsional barriers with umbrella sampling. *J. Chem. Theory Comput.* **2011**, *7*, 2989–3000.

(38) Sasada, T.; Reinherz, E. L. A critical role for CD2 in both thymic selection events and mature T cell function. *J. Immunol.* **2001**, *166*, 2394–2403.

(39) Tibaldi, E. V.; Salgia, R.; Reinherz, E. L. CD2 molecules redistribute to the uropod during T cell scanning: Implications for cellular activation and immune surveillance. *Proc. Natl. Acad. Sci. U.S.A.* **2002**, *99*, 7582–7587.

(40) Bogan, A. A.; Thorm, K. S. Anatomy of hot spots in protein interfaces. *J. Mol. Biol.* **1998**, *280*, 1–9.

(41) Kim, M.; Sun, Z. J.; Byron, O.; Campbell, G.; Wagner, G.; Wang, J.; Reinherz, E. L. Molecular dissection of the CD2-CD58 counter-receptor interface identifies CD2 Tyr86 and CD58 Lys34 residues as the functional “hot spot”. *J. Mol. Biol.* **2001**, *312*, 711–720.

(42) Swaminathan, S.; Harte, W. E., Jr.; Beveridge, D. L. Investigation of domain structure in proteins via molecular dynamics simulation: application to HIV-1 protease dimer. *J. Am. Chem. Soc.* **1991**, *113*, 2717–2721.

(43) Arnold, G. E.; Ornstein, R. L. Molecular dynamics study of time-correlated protein domain motions and molecular flexibility: cytochrome P450BM-3. *Biophys. J.* **1997**, *73*, 1147–1159.